Fundamental investigation of foam flow in a liquid-filled Hele-Shaw cell

Kofi Osei-Bonsu[1], Nima Shokri[1]*, Paul Grassia[2,3]

[1]School of Chemical Engineering and Analytical Science, University of Manchester, Manchester, UK

[2] Department of Chemical and Process Engineering, University of Strathclyde, James Weir Building, 75 Montrose St, Glasgow G1 1XJ, UK

[3]Ciencias Matemáticas y Físicas, Universidad Católica de Temuco, Rudecindo Ortega 02950, Temuco, Chile

*Corresponding author

Dr. Nima Shokri

School of Chemical Engineering and Analytical Science

Room C26, The Mill

The University of Manchester

Sackville Street, Manchester, M13 9PL, UK

Tel: 0441613063980

Email: nima.shokri@manchester.ac.uk

Group website: http://personalpages.manchester.ac.uk/staff/nima.shokri/

Abstract

The relative immobility of foam in porous media suppresses the formation of fingers during oil displacement leading to a more stable displacement which is desired in various processes such as Enhanced Oil Recovery (EOR) or soil remediation practices. Various parameters may influence the efficiency of foam-assisted oil displacement such as properties of oil, the permeability and heterogeneity of the porous medium and physical and chemical characteristics of foam. In the present work, we have conducted a comprehensive series of experiments using customised Hele-Shaw cells filled with either water or oil to describe the effects of foam quality, permeability of the cell as well as the injection rate on the apparent viscosity of foam which is required to investigate foam displacement. Our results reveal the significant impact of foam texture and bubble size on the foam apparent viscosity. Foams with smaller bubble sizes have a higher apparent viscosity. This statement only applies (strictly speaking) when the foam quality is constant. However, wet foams with smaller bubbles may have lower apparent viscosity compared to dry foams with larger bubbles. Furthermore, our results show the occurrence of more stable foam-water fronts as foam quality decreases. Besides, the complexity of oil displacement by foam as well as its destabilizing effects on foam displacement has been discussed. Our results extend the physical understanding of foam-assisted liquid displacement in Hele-Shaw cell which is a step to ~~required to~~ understanding the foam flow behaviour in more complex systems such as porous media.

1. Introduction

Foams demonstrate great potential for displacing liquid in porous media which is relevant to a variety of processes such as the Enhanced Oil Recovery (EOR) or soil remediation practices. The underlying reason behind the application of foam in these processes is its ability to reduce significantly the mobility of gas in porous media [1-4]. For example, substantial amounts of oil initially in place remain unproduced from reservoirs after the first phase of oil recovery; the so-called primary recovery [5-8]. Gases such as nitrogen, carbon dioxide and air are typically injected into the reservoir to displace the remaining hydrocarbons. However, the overall sweep efficiency is still considerably low due to the poor gas contact with the oil in the reservoir [9,10]. This effect is attributed to gravity override and viscous fingering associated respectively with the density and viscosity contrast between the injected gas and the reservoir fluids [6,11].The presence of heterogeneity in reservoirs further aggravates these defects by channelling; whereby the injected gas preferentially flows through the high permeability streaks of the reservoir leaving much of the oil behind [12,13]. The cumulative effect of these challenges may result in a premature gas breakthrough, thereby rendering the utilization of gas ineffective.

Application of foam has proven to be a potential remedy for improving the effectiveness of the gas flooding process [14-19]. Foam is defined as a dispersion of gas in a continuous liquid phase. For effective utilization of foam, it is necessary to understand its behaviour under different boundary conditions and quantify the effects of various parameters on its performance. Consequently, many studies have been undertaken at different length scales to investigate different aspects of foam dynamics in porous media; from generation to propagation to destruction [2, 20,21].

67 The relative immobility of foam in porous media reduces the fingering phenomena providing
68 a more favourable displacement of oil [22, 23]. Foam reduces gas relative permeability by
69 trapping gas in the porous medium which effectively reduces the number of flow paths for
70 the flowing gas [20, 24,25,26]. The gas relative permeability reduces also as a result of the
71 increase in the effective viscosity (or apparent viscosity) caused primarily by the liquid films
72 in foam which create resistance to flow.

73 Ma et al. [26] conducted experiments to investigate the performance of foam in a
74 heterogeneous micromodel in the absence of oil. They observed improved sweep efficiency
75 by foam and a substantial gas diversion from the high permeability section to the low
76 permeability section of the micromodel. They also recorded longer breakthrough time during
77 displacement as the foam quality increased until a critical point above which increasing foam
78 quality (i.e. gas volume fraction) resulted in a decrease in the gas break-through time. A
79 similar experiment was taken a step further by investigating the effects of the presence of a
80 non-aqueous phase on the foam performance [16]. The results demonstrated the ability of
81 foam to improve oil recovery as well as sweep efficiency compared to air and water. Prior to
82 these recent micro-model studies, others had observed this phenomenon in core flooding
83 experiments in the presence of the permeability contrast [15,27,28]. For example, Casteel and
84 Djabbarah [27] evaluated the performance of foam and water-alternating-gas in two parallel
85 Berea cores differing in the permeability. They observed that foam generation was favourable
86 in the core with higher permeability and that allowed CO_2 diversion into the core with the
87 lower permeability. Bertin et al. [28] observed similar phenomena in sand-packs with very
88 high permeability contrasts.

89 In addition to the ability of foam to divert gas and eliminate preferential flooding or
90 channelling, the presence of foam significantly reduces the gas mobility or equivalently
91 increases the gas apparent viscosity. The apparent viscosity according to Hirasaki and

Lawson [25] is a sum contribution of three elements: (i) the viscosity of the liquid slugs between the gas bubbles, (ii) the resistance due to interface deformation and (iii) the resistance to flow caused by surface tension gradient in bubbles. The apparent viscosity may be estimated using the Darcy's law or Plane-Poiseuille or cylindrical–poiseuille flow in the case of Hele-Shaw cells or capillary tubes respectively [32].

Experiments have revealed that apparent viscosity depends o~~f~~n foam quality (i.e. gas fraction), foam texture (i.e. bubble size), injection flow rate as well as permeability of the medium [15,25,29,30,31]. Table 1 presents key findings of some relevant papers. Llave et al. [15] investigated the resistance factors of flowing foams in bead-packs as a function of foam quality and injection rate. They concluded that mobility of foam reduces (i.e. increase in apparent viscosity) as the foam quality increases. Furthermore, they observed a shear thinning behaviour between injected flow rate and foam mobility such that low shear rates resulted in higher resistance to flow of gas. Minssieux [31] observed an increase in foam viscosity (i.e. a reduction in foam mobility) with increasing foam quality when the viscosity of the foams were measured with a viscometer (no porous medium) but observed the opposite when the foam viscosity was -calculated from the effluent flow rate of foam in porous media. Marsden et al. [30] however, recognised that the foam texture, defined by the bubble size rather than the gas fraction (foam quality) was the principal control on foam mobility. They observed that high foam quality, characterised by bigger bubbles, increased the apparent viscosity (i.e. reduced the mobility) of foam in agreement with the results presented in Llave et al. [15]. Hirasaki and Lawson [25] conducted a systematic series of experiments to investigate the effect of several parameters such as foam texture, foam quality, gas velocity and capillary radius on the apparent viscosity of foam. They concluded that foam texture or bubble size was the principal variable affecting the apparent viscosity of foam flowing through capillaries. Yan et al. [32] conducted similar experiments to investigate the effect of different

parameters on apparent viscosity in a Hele Shaw cell. They again concluded that, foam texture is the main factor that determines the number of lamellae per unit length which is the principal factor affecting the foam viscosity.

Table 1: Summary of key literature

Reference	Key observation/conclusion
Llave et al. (151990)	Decrease in foam mobility with increasing foam quality and decreasing flowrate.
Minssieux et al. (197431)	Mobility decreases as foam quality increase (viscometer). Foam mobility decreased as quality decreased in porous medium (viscosity measured from effluent flow rate).
Marsden et al. (196730)	Foam mobility is controlled by foam texture (i.e. bubble size)
Hirasaki and Lawson (198525)	Foam texture determines whether foam exist as bulk foam or lamellae. Foam texture is the key parameter that affects mobility of foam
Yan et al. (200632)	Foam texture is the main determinant of the number of lamellae per unit length – the principal factor affecting the foam apparent viscosity.

In spite of numerous studies conducted on foam, the relationship between foam quality, foam texture or bubble size and apparent viscosity is still not very well-understood due to its complexity [20,29,33,34]. Furthermore, foam texture is actually affected by many other parameters such as the capillary pressure, bubble velocity, injection rate, surfactant concentration and also the foam generation and coalescence mechanism, adding to the complexity of the relationship between texture and foam apparent viscosity [29,34,35]. Motivated by the important application of foam in EOR as well as remediation practices, the

specific objective of this study was to extend the understanding of the parameters influencing the apparent viscosity of foam under well-controlled boundary conditions. To do so, we have undertaken a comprehensive series of experiments to investigate the relationship between foam quality, bubble size, cell permeability and apparent viscosity and evaluate their relative importance with respect to each other. We chose Hele-Shaw cell geometry because it was particularly easy to obtain images of the foams and to determine the bubble size in this geometry. The rest of the paper is laid out as follows: Section 2 provides a detailed description of the experimental setup and the procedure used in this study. Section 3 presents the findings and analysis of the results from the experiments and in Section 4 the final conclusions derived from the study are presented.

2. Experimental considerations

The apparent viscosity of foam and the displacement dynamics were quantified in a 2D Hele-Shaw cell as illustrated in Figure 1. The cell was constructed from two glass plates with dimensions of 31 x 20 x 0.6 cm. The two glass plates were fixed into a Plexiglas frame. The surface of the plates was polished to eliminate any surface irregularities. A gasket of thickness 0.05 cm (unless otherwise specified) was clamped between the two glass plates to create gap (in this study we used three gaskets differing in thickness to evaluate the effects of the gap thickness (cell permeability) on the foam performance). The gasket also acted as a seal to prevent leakage. A perforation was made 2 cm away from the edges of the top Plexiglas frame to create an inlet and outlet of fluid into and out of the cell. At the injection point, the gasket was V-shaped to ensure uniform entry of the pre-generated foam into the Hele-Shaw cell.

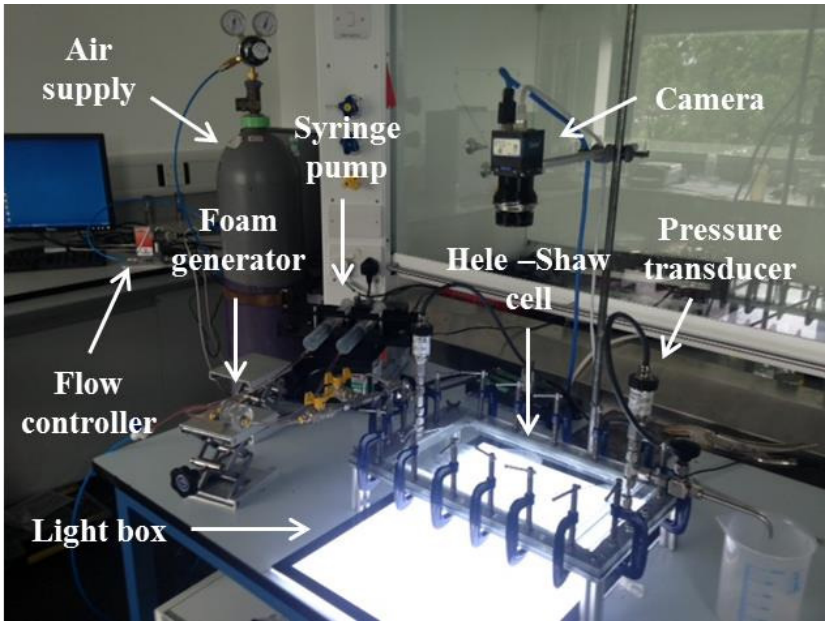

Figure 1. Experimental setup used to investigate liquid displacement by foam. The customised Hele Shaw cell was made up of borosilicate glass plates of dimensions 32 x 20 cm. A thin gasket of thickness 0.05 cm was sandwiched between the two plates to create a gap. The cell was initially filled with water after which foam was injected. The syringe pump and the gas flow controller were used to inject the surfactant solution and the gas respectively through the foam generator to create foam. The camera was used to record the dynamics of the displacement process.

Foam was generated by injecting air and surfactant solution simultaneously through a customised foam generator with a sintered glass disc (Glass Scientific, UK) fitted in it. The surfactant solution was injected at a controlled flow rate by a syringe pump (Harvard Apparatus, USA) and the air was controlled by a Mass flow controller (Bronkhurst, UK). Foam was generated as the surfactant solution and the air converged and passed through the sintered disc. The generated foam entered the Hele-Shaw cell directly from the foam generator (via a tubing of internal diameter 0.4 cm) to displace the fluid in it. Despite the confined geometry of the Hele-Shaw cell, the process of transferring bubbles from the tubing into the cell did not appear to either break up bubble or coalesce them (which could also be checked by varying the gap thickness in the Hele-Shaw cell about the default thinness 0.05 cm, and verifying that for a given foam quality the observed bubble area viewed from above

169 the Hele-Shaw cell scaled inversely with the gap thickness). Pressure transducers were
170 connected to the inlet and outlet of the Hele-Shaw cell to measure the differential pressure of
171 the foam as it moved through the cell.

172 The surfactant solution used in the experiments consisted of 2% active content of 1:1 mixture
173 of Sodium dodecyl sulphate (Sigma Aldrich) and Cocamidopropyl betaine (The Soap
174 Kitchen). This surfactant combination demonstrates high stability in the absence and presence
175 of oil in the previous studies [36,37]. A monochromic camera with a resolution of 2560 x
176 2042 pixels was mounted above the Hele-Shaw cell as shown in Figure 1, to record the
177 dynamics of the displacement process at well-defined time intervals. A light box was placed
178 under the Hele-Shaw cell to enhance the illumination and the quality of the recorded images.

179 We conducted four different experiments in this study. First, the effect of foam quality on the
180 apparent viscosity of foam was investigated. The experiments were conducted for foam
181 qualities between 81 and 99%. Pressure drop within this regime is independent of gas
182 flowrate [38] hence the foam quality was controlled by changing the liquid (surfactant
183 solution) flowrate. The gas flow rate was 10 ml/min in all experiments unless otherwise
184 specified. Two different foam generators labelled fine and coarse with pores size distribution
185 16-40 micron and 40-100 micron respectively were used. The purpose of this was to modify
186 the bubble size. Second, the effect of the foam flow rate on the apparent viscosity was also
187 investigated. This was done by choosing a fixed foam quality and changing the total volume
188 flow rate of the foam for gas flow rates between 10 and 60 ml/min and changing the
189 surfactant flowrate accordingly. Third, the effect of gap thickness on the apparent viscosity of
190 foam was also investigated by changing the gasket thickness. This was conducted for 3 gap
191 sizes; 0.03, 0.05 and 0.1 cm. In the above mentioned experiments, the displaced phase was
192 water. The effect of foam quality on the velocity profiles (displacement front) was analysed
193 and the displacement efficiency was investigated. A final experiment was conducted to show

194 the effect of the presence of oil (a non-aqueous phase) on the foam performance and the
195 displacement dynamics and the challenges associated with the foam in the presence of oil.
196 For this experiment, the Hele Shaw cell was fully filled with a silicon oil (Dow Corning 200)
197 of viscosity 100 centistokes before injecting foam to displace it. Each experiment was
198 repeated several times (at least three times) to ensure repeatability.

199 We used Image J (image processing software) to analyse the recorded images and delineate
200 the dynamics of the process. The grey-scale images were segmented into black and white.
201 Different algorithms were used to extract the required information such as the average bubble
202 size and the velocity profiles from the images. The image analysis technique was similar to
203 the procedure explained in Osei-Bonsu et al. [37] thus it is not repeated here. Figure 2
204 illustrates a typical grey-scale image recorded by the camera during the displacement
205 experiment with the corresponding black and white image.

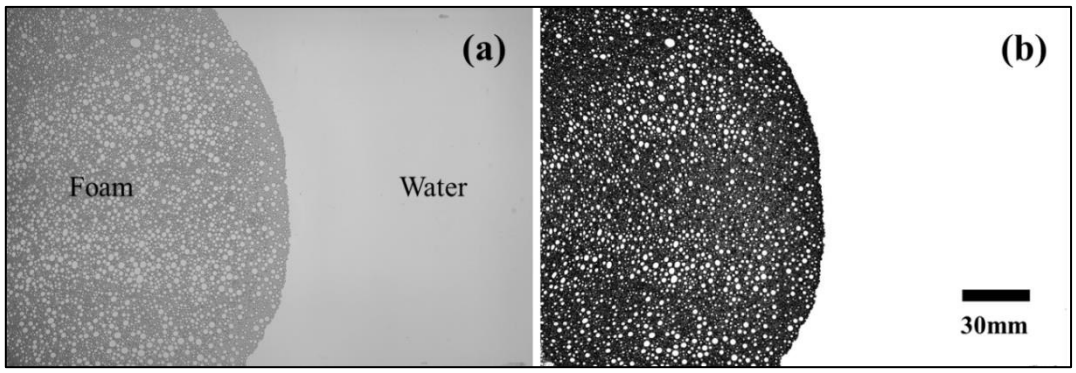

206

207 **Figure 2**. (a) A typical gray-scale image recorded by the CCD camera, (b) the corresponding black and white
208 image indicating foam films (lamellae) and dispersed gas represented by black and white, respectively.

209 ## 3. Results and discussions

210 ### 3.1. Effect of foam quality on the apparent viscosity

211 Figure 3 shows qualitatively the patterns of the foam with the quality of 99% and 81%
212 indicating the dry and wet foam respectively.

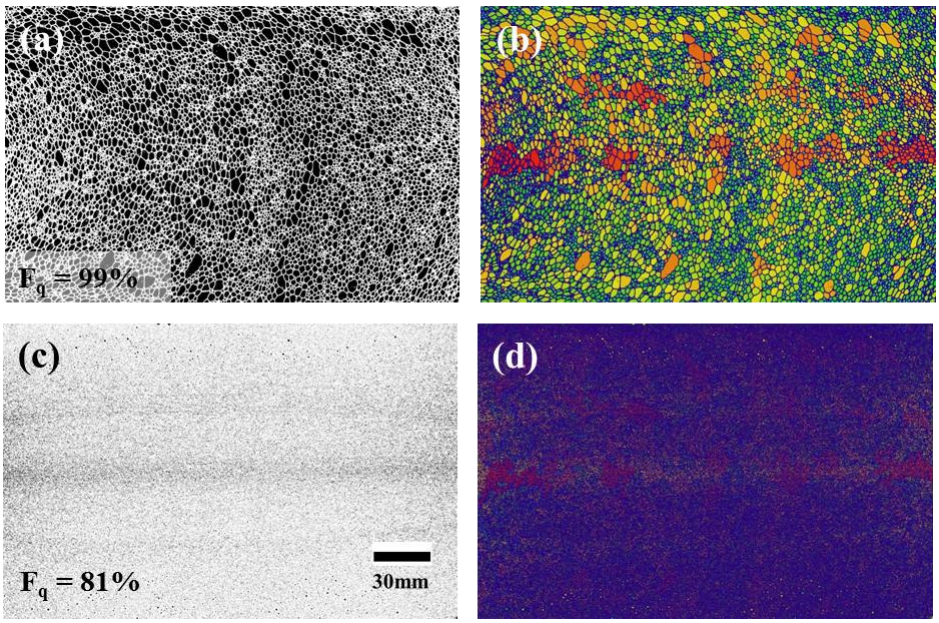

Figure 3. Two segmented images with the corresponding bubble size distribution map for the foam with the highest (a,b) and lowest (c,d) foam quality representing the dry and wet foam, respectively. F_q is the foam quality (i.e. gas fraction).

Figure 3 shows that foam with low quality (i.e. high liquid content) contains smaller bubbles with a narrower bubble size distribution. To quantify the foam apparent viscosity as a function of foam quality, we employed the plane-Poiseuille equation [32] using the measured pressure drop across the Hele – Shaw cell given by the following equation:

$$\mu_{fapp} = \frac{k\Delta P}{qL} = \frac{b^2\Delta P}{12qL} \quad (1)$$

where μ_{fapp} is the apparent viscosity of foam, $k = \frac{b^2}{12}$ is the permeability (b is the gap thickness of the Hele Shaw cell), q is the velocity of the foam (i.e. the volumetric flow rate divided by the cross-sectional area of the Hele-Shaw cell), L is the length of the Hele-Shaw cell and $\frac{\Delta P}{L}$ is the pressure gradient across the Hele-Shaw cell.

Figure 4 shows the obtained relationship between the foam quality and apparent viscosity. The results show that the apparent viscosity of foam increases as foam quality increases. It is

known that for bulk foams, foams with higher gas fraction (high quality) require more deformation to yield and flow hence have higher yield stress and subsequently expected to have lower mobility. [39,40]. On the contrary, when the foam quality is low, wet foams are produced. Wet foams are more mobile than dry foams because the bubbles in wet foams are more spherical and uniform hence there is very small interference between bubbles resisting flow [47]. The viscosity of the wet foams however is still significantly higher than the viscosities of their constituents (the air and the surfactant solution). Also according to Cantat [41], foam flow in ~~porous media~~confined geometries is controlled by the movement of foam meniscus along the surface of the medium confining the foam. This high viscosity can therefore be ascribed to the high dissipation in dry foams due to the close contact between the Plateau borders and the wall of the medium [41,42].

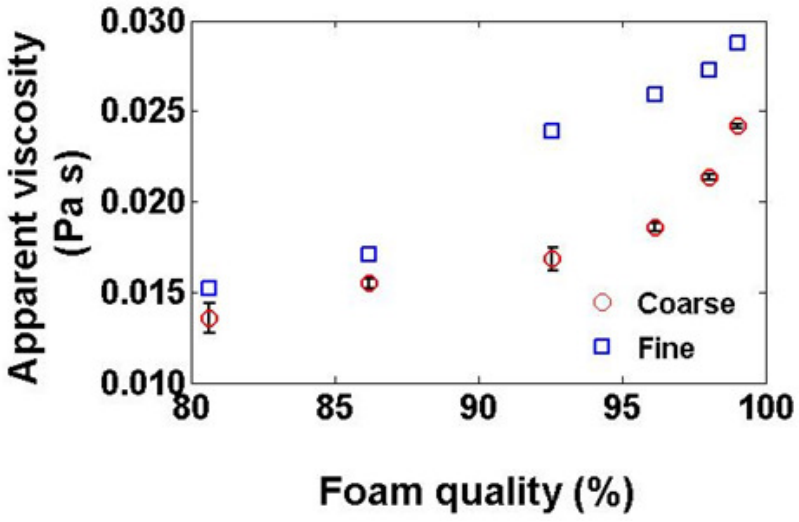

Figure 4. The relationship between foam quality, foam generator pore size and apparent viscosity of foam. The results for two foam generators labelled as coarse and fine in the legend with the pore size distribution of 40-100 microns and 16-40 microns, respectively are shown. The bubbles generated by fine size foam generator were smaller than that of the coarse foam generator. The error bars represent the standard deviation of the repeated tests. ~~Apparent viscosity of foam increases with increasing foam quality. For the same foam quality, the apparent viscosity increases with decreasing the pore size of the foam generator.~~

245 It is generally believed that foam texture defined by the number of bubbles per unit area or
246 bubble size is the dominant parameter controlling the apparent viscosity of foam [20,32,43].
247 Using the segmented images, we could investigate the relationship between foam quality,
248 bubble size and the apparent viscosity with the results presented in Figure 5. Note that the
249 bubble size discussed here is the bubble size observed by the camera positioned above the
250 cell. Our results show that, for the same foam generator (sintered glass disc of defined pore
251 size distribution), foam at low quality is generally characterised by finer bubbles and hence
252 more bubbles per unit area while bigger bubbles are generally generated at higher quality.
253 This phenomenon was observed by others as well [15, 26, 30, 33]. The reason for this
254 behaviour is ascribed to the volumes of dispersed gas per unit volume of surfactant solution
255 injected (i.e. the higher the gas fraction or foam quality, the higher the volume of dispersed
256 gas per unit volume of the surfactant solution injected). See Figure A in the Appendix (where
257 the foam quality is plotted against liquid volume per bubble). These results suggest that,
258 higher bubble number density (number of bubbles/unit area) does not necessarily equate to
259 the higher apparent viscosity (as the higher bubble number density might be associated with
260 lower foam quality). Figure 5(b) shows a direct relationship between the average bubble sizes
261 of the foam generated at different gas fractions with their corresponding apparent viscosities
262 for the two foam generators of different pore size distributions.

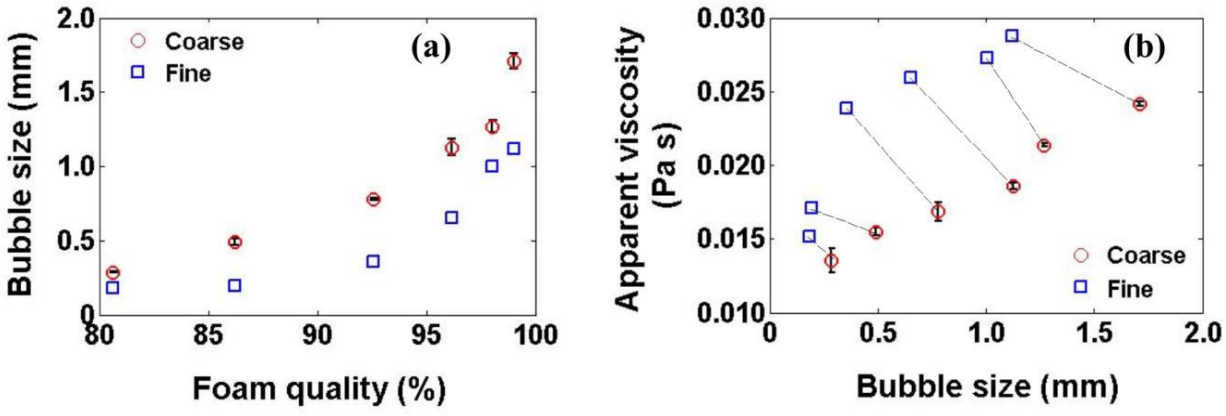

263

Figure 5. (a) The bubble size as a function of foam quality (i.e. gas fraction) for foam generated by coarse (40-100 microns) and fine (16-40) foam generators (b) the relationship between the apparent viscosity and the average bubble size of the foams produced by the coarse and fine foam generators.~~.~~ The dashed ~~lines in (b) represents~~lines in (b) represent loci of constant foam quality (merely to guide the eye). ~~As the foam quality decreases, foams with smaller bubble sizes are generated.~~

Also it can be noticed from Figure 5 that the average bubble size (i.e. defined as the equivalent diameter of a circle with the same area as the bubble) at lower end of foam quality used in our experiments (81 and 86%) is lower than the gap spacing of the Hele-Shaw cell. This affects the shape of the bubbles compared to other higher foam qualities in which the bubbles are flattened by the confining plates. This flattening increases the interaction between the bubbles and the confining plates, subsequently influencing the apparent viscosity.

We conclude that the apparent viscosity of foam depends on the foam quality such that the drier the foam the higher the apparent viscosity (given that the foam is stable and that the bubbles do not coalesce or rupture). However, for a given foam quality, foam with finer texture or smaller bubble size has higher apparent viscosity as shown in Figure 4. This is because foam containing smaller bubbles require more stress to be deformed (higher deformational stress implies higher viscosity). Moreover, since dissipation in foams flowing in ~~porous media~~confined geometries involves motion of liquid meniscus along the ~~porous~~ confining medium, smaller bubbles will have more total length of menisci per total area than larger ones resulting in a higher resistance to flow and hence higher viscosity [41,44].

3.2 Effects of foam flow rate on the apparent viscosity

We investigated the effect of foam flow rate on the apparent viscosity. To do so, the foam quality was maintained constant while increasing the foam flow rates. This test was conducted under the foam qualities of 98% and 93%. According to Figure 6 the apparent viscosity of foam decreases with increasing gas flow rate. This conclusion is in agreement

289 with the results presented in other studies [25,32,43]. For the foam of the same gas fraction,
290 increasing the foam flowrate effectively increases the shear stress and the shear rate but the
291 latter will increase quicker than the former subsequently leading a decrease in foam viscosity.
292 Figure 6 also shows that decreasing foam quality results in a lower apparent viscosity as
293 discussed in Section 3.1.

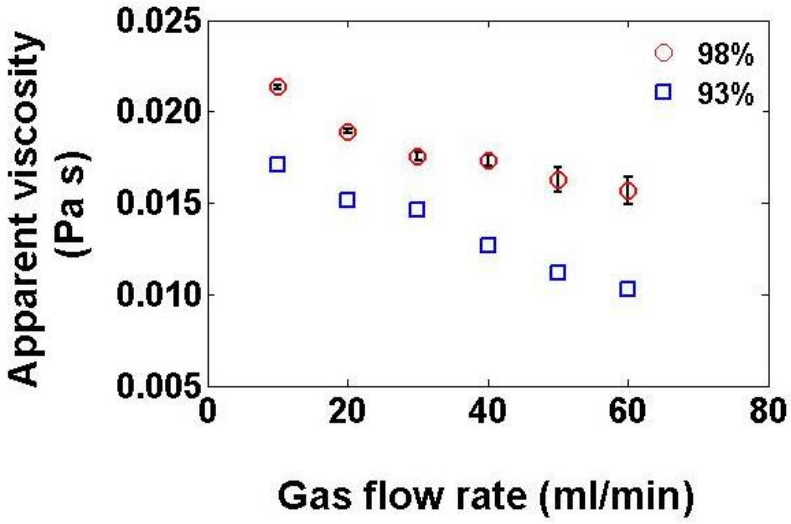

294

295 **Figure 6.** The relationship between the gas flowrate and the apparent viscosity for foam qualities of 98% - circle
296 and 93% - square. Apparent viscosity of foam decreases with increasing flowrate and decreases with decreasing
297 foam quality.

298 **3.3 Effects of the gap thickness on the apparent viscosity**

299 Using the developed experimental setup, we could investigate the effect of the gap size
300 (defining the permeability of the cell) on the apparent viscosity. In this study two foam
301 generators were used in order to elucidate the effect of bubble size (at constant foam quality)
302 on the apparent viscosity of foam. The results in Figure 7 show that foam apparent viscosity
303 increases with the gap size.

304 Analysis presented in Cantat [41] enables one to estimate the stress associated with a foam
305 moving through a porous medium in terms of the length of menisci per unit surface area of

306 the confining medium and also the speed of the menisci (expressed as a capillary number).
307 Increasing the gap thickness (for a fixed volumetric flow rate) reduces the speed and this
308 tends to decrease the stress. The effect of the gap thickness upon the length of menisci per
309 area is harder to predict though being sensitive to bubble shape. For bubbles that are highly
310 flattened, increasing the gap thickness decreases length of menisci and also decreases bubble
311 contact area with the medium, but the latter decreases more quickly than the former, so the
312 ratio between them increases. For bubbles that are small enough to fit between the plates
313 without much flattening, moving plates apart might cause contact on one or other plate to be
314 lost altogether (and the associated menisci might likewise be lost), but the bubble is still
315 observed to occupy a finite area when viewed from above or below the plates. Aside from
316 these complex effects governing the stress, increasing the gap thickness also tends to reduce
317 the apparent strain rate (scaling as the ratio between the speed of the menisci and plate
318 spacing). Apparent viscosity (stress divided by strain rate) should thereby increase. Figure 7
319 shows that for the same foam quality, the apparent viscosity increases as the bubble size
320 decreases as previously discussed in section 3.1.

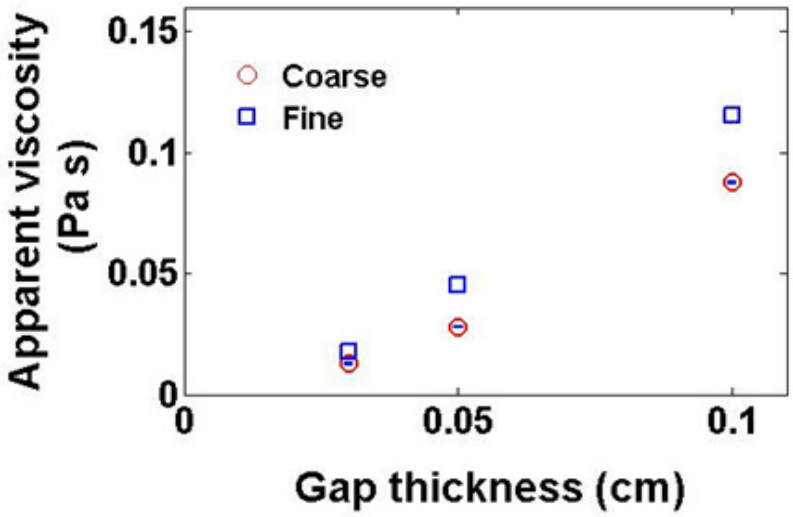

321

322 **Figure 7.** The relationship between the gap thickness and apparent viscosity of foam for two foam generators
323 characterised by different pore size distribution. The foam generator with the pore size ranges of 16-40 microns,

and 40-100 microns are referred as Fine and Coarse in the legend. ~~Moving the plates apart resulted in increase in apparent viscosity of foam.~~

3.4 Dynamics of foam displacement

When foam quality changes, the apparent viscosity of foam is modified as shown in previous figures. This will eventually affect the dynamics and patterns of the interface separating foam from the displacing fluid. Figure 8 qualitatively shows the patterns and dynamics of foam front displacement as influenced by the foam quality. The interface between foam and water was traced at the selected time steps. These traced interfaces were then superimposed as presented in Figure 8 depicting the profiles of air (a) and foam of quality 98% (b), 96% (c) and 81 % (d). In the case of air, the time-step between each profile is 15 seconds while it is 25 seconds in the other three cases.

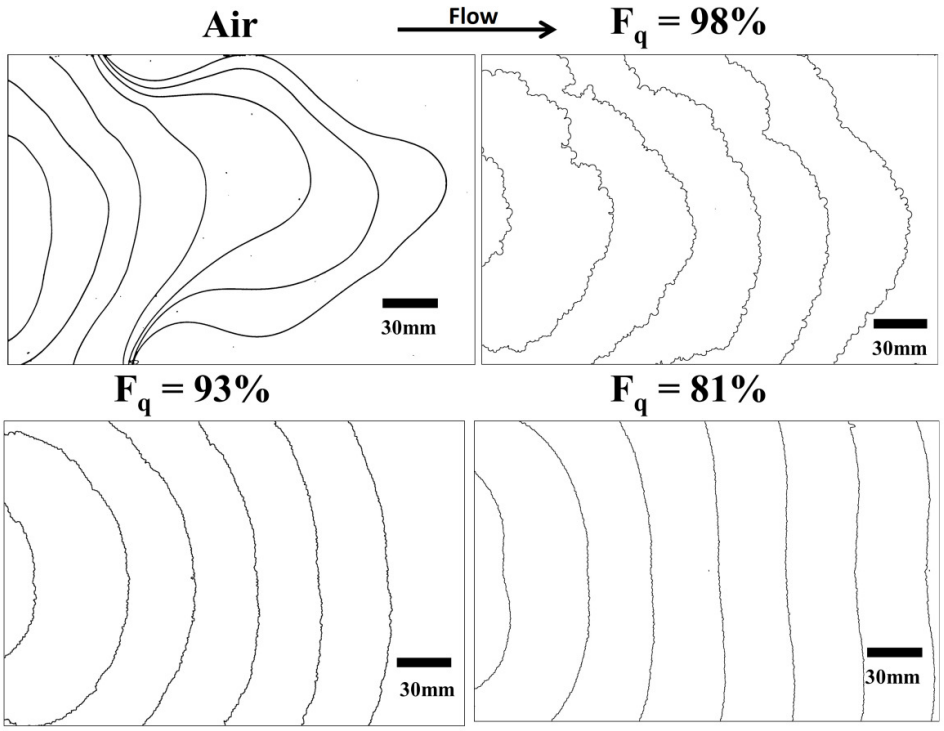

Figure 8. The interface between the displacing and displaced fluid represented at equal time intervals propagating from left to the right. F_q indicate foam quality. The displacing fluid in (a) is air and the time interval between each interface is 15 seconds and the displacing fluid is foam with the quality of 98% in (b), 93% in (c)

and 81% in (d). The arrow in the figure shows the flow direction. The time interval between each interface in (b-d) is 25 seconds. This figure shows that applying foam reduces the mobility of gas leading to more stable displacements. It can also be observed that as the foam quality decreases, the foam front becomes more uniform.

It must be clarified here that, the total volume flow rate in the case of the foams (gas plus surfactant solution) is slightly higher than the flow of air alone. According to our results, the mobility of gas was noticeably reduced by the presence of surfactant solution (i.e. when it is foamed). The gas flow rate is 10 ml/min in all the cases presented in Figure 8. The presence of foam delayed gas breakthrough by more than 45 seconds in each case. Also unlike air which resulted in no further water displacement after gas breakthrough, foam (even at 99% foam quality) recovered all the water in the cell before breakthrough which confirms the great potential of foam in reducing or eliminating the detrimental effects of fingering during immiscible displacement in a Hele-Shaw cell~~porous media~~.

3.5 Efficiency of foam flooding as influenced by foam quality

In this section, we discuss the displacement efficiency as a function of the foam quality. Displacement efficiency was quantified in terms of the cumulative liquid (surfactant solution) injected and recovery factor (given by the fraction of the total volume of liquid displaced to the initial volume of liquid in the Hele-Shaw cell). The results are presented in Figure 9 showing that although increasing the liquid fraction (resulting in low foam quality) leads to a stable displacement interface (as shown in Figure 8), the efficiency of the displacement decreases as the foam quality decreases. This is because more surfactant is utilized in the displacement process to achieve a fixed recovery factor. It must be noted here that when total foam volume is plotted against the recovery factor, all the lines in the graph collapse on top of each other. This means that as far as foam water displacement is concerned, the recovery efficiency is identical (i.e. regardless of the foam quality). ~~This conclusion may be altered in~~

~~the case of porous media or fluids with different properties than the one used in the present study.~~

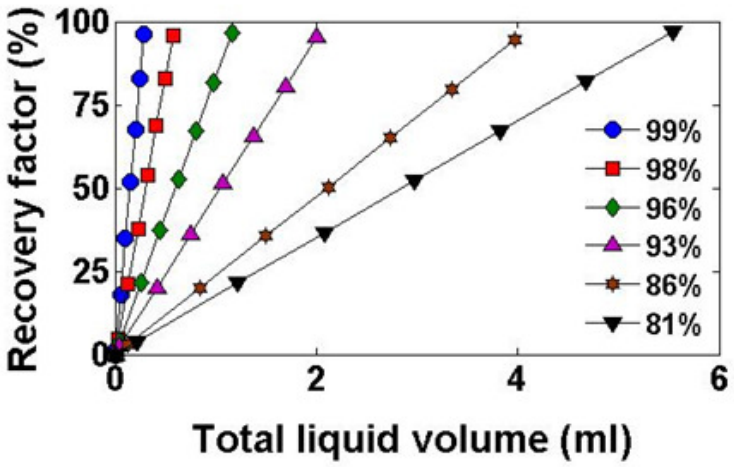

Figure 9. The recovery efficiency of foams with different qualities (gas fractions) as presented in the legend. The total liquid volume represents the cumulative volume of surfactant solution used to displace water. ~~The higher the foam quality, the more efficient the displacement process as less surfactant solution is used in the displacement process.~~

3.6 Challenges present in foam-oil displacement

One of the major deterrents to the progress of foam application in EOR is the negative influence of oil [45] on foams. It has been reported that the presence of oil reduces the stability of the foam which could hinder the effectiveness of the displacement process and hence the recovery efficiency [31,37,46]. We present here a qualitative visualisation of the foam-oil interaction during foam-oil displacement in a Hele-Shaw. The silicone oil used in this study had a viscosity of 100 centistokes. Two foams with the quality of 98% (dry) and 81% (wet) were used to investigate the oil displacement by foam. Figure 10 illustrates the observed displacement patterns. This figure shows that the presence of oil in the Hele-Shaw cell significantly influenced the stability of foam. While the bubble sizes in the foam were consistent throughout the Hele-Shaw cell in the case of water displacement, the presence of

oil altered the bubble size of the foam leading to the formation of large bubble particularly near the interface between the oil and foam. These big gas bubbles represent the volumes of air that escaped from the foam network due to coalescence and rupturing of the bubbles in the presence of oil. Furthermore, it was observed that the tolerance of the foam to oil destruction increases as the foam quality decreases. This is because the foam films and the Plateau borders produced at low foam quality are thicker (relative to the bubble size) than the films and borders generated when the gas fraction is high. The thicker films are able to supress the penetration of oil into the gas-liquid interface of the foams. In addition, the thicker borders imply less capillary suction pressure draining the films. The length of the films (relative to the total bubble perimeter) is moreover less for low quality foam, meaning oil is less likely to find its way to the film in the first place.

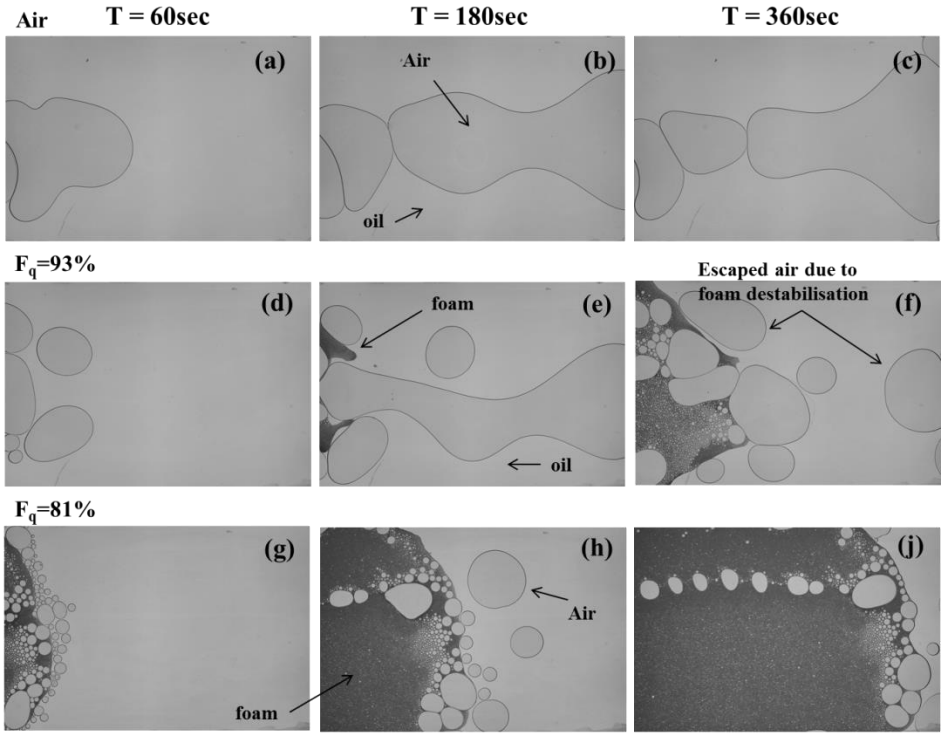

Figure 10. Displacement of oil by air (a-c), foam with the quality of 93% (d-f) and foam with the quality of 81% (g-f). These figures show that generally foam improves oil recovery compared to air. Also, for the foam with the quality of 93%, the destabilizing effect of oil is more pronounced compared to the case of the foam with the quality of 81%.

In the case of the high quality foam, although oil destabilizes the foam heavily in the initial stage, stable foams eventually formed and all the oil in the Hele-Shaw cell was displaced. Although oil effect on the foam destabilization was well pronounced in this case, it was nonetheless still more effective than the scenario where pure air was applied. After gas breakthrough in the latter case, additional air injection resulted in negligible oil recovery.

4. Summary and conclusions

We have conducted a series of experiments to investigate the parameters that control foam apparent viscosity and foam water (as well as oil) displacement in Hele-Shaw cells. This study extends the physical understanding of the parameters controlling foam flow in Hele-Shaw cell under different boundary conditions. ~~This is required to understand the process under more complex systems~~. Based on the obtained results, following observations and conclusions can be made:

1. Apparent viscosity depends on the foam quality, bubble size, foam flow rate and gap thickness.
2. Dry foams (high foam quality) provide more resistance to the flow of gas (i.e. reduces gas mobility) than low quality foam characterised by high liquid content.
3. For the same foam generator, an increase in foam quality resulted in an increase in average bubble size. This is because more volume of air is dispersed per volume of surfactant solution as the gas fraction increases.
4. Apparent viscosity of foam does not increase with bubble size indiscriminately but depends also on the foam quality. Wet foams with smaller average bubble size may have a lower apparent viscosity than dry foam with a bigger average bubble size. However, for the same foam quality, decrease in the bubble size results in an increase in the apparent

viscosity as the shear stress required for bubble deformation and the total length of the meniscus (per unit total area) increase.

5. The presence of oil affects the stability of foam during foam oil displacement. The degree of destabilisation may vary according to the foam quality used in the displacement. Low foam quality with smaller bubbles is more resistant to the adverse effect of oil.

Study of foam flow in a Hele – Shaw cell is a first step towards understanding the foam flow process in more complex systems (e.g. porous media). However, very complex and additional phenomena occur in porous media which are absent from our Hele-Shaw experiments such as capillary pressure effects, bubble coalescence and in situ foam generation [1, 48]. One system in which Hele-shaw cell flows may nonetheless become particularly relevant to oil recovery is in the case of fractured porous media [35] in which case Hele-Shaw cell might be considered analogous to foam flow in fractures.

Appendix

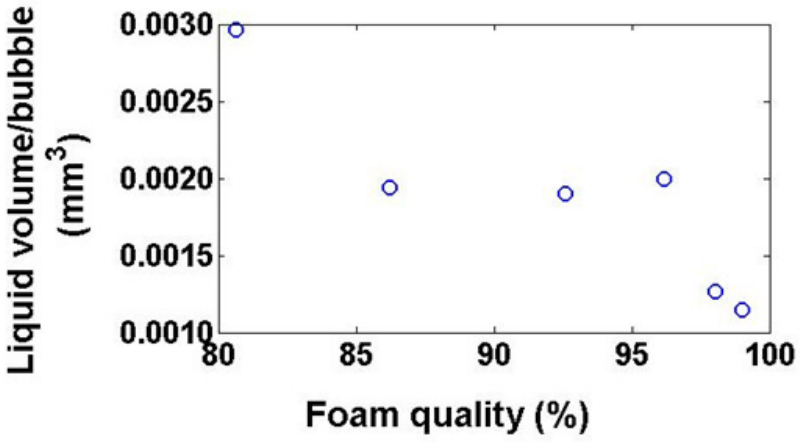

Figure A. The liquid volume per bubble as a function of the foam quality. Unlike bubble gas volume in foam that increase drastically as foam quality increases (reflected in the average bubble size) the amount of variation of liquid volume per bubble is comparatively small though the trend is not as simple as the case of the gas volume.

438 **Acknowledgments**

439 Nima Shokri would like to acknowledge the donors of the American Chemical Society
440 Petroleum Research Fund for partial support of this research (PRF No. 52054-DNI6) and the
441 equipment funding from The Royal Society (RG140088). Paul Grassia acknowledges
442 sabbatical stay funding CONICYT Chile (folio 80140040). We would like to acknowledge
443 the UK Engineering and Physical Sciences Research Council (EPSRC) to provide the PhD
444 studentship (EP/L504877/1) for Kofi Osei-Bonsu. We would like to thank Mr. Craig Shore,
445 Ian Small and Mr. Andrew Evans for their assistance with the experimental setup.

446 **References**

447 [1] P. A Gauglitz, F. Friedmann, S.I. Kam, and W.R. Rossen, Chem. Eng. Sci. 57 (2002)
448 4037-4052.

449 [2] G. Hirasaki, Soc. Petrol. Eng. J. (1989) SPE 19518.

450 [3] A. R. Kovscek, T.W. Patzek, and C.J. Radke, Soc. Petrol. Eng J. 2 (1997) 511-526.

451 [4] A.R. Kovscek, and H. Bertin, Transport Porous Med. 52 (2003) 17-35.

452 [5] A. Payatakes, Ann. Rev. Fluid Mech. 14 (1982) 365-393.

453 [6] D. W. Green, and G.P. Willhite, Enhanced Oil Recovery in SPE Textbook Series, Vol 6,
454 (1998) Richardson, TX.

455 [7] L.W. Lake, and P. B. Venuto, Oil Gas J. 88 (1990) 62-67.

456 [8] M. Sahimi, Flow and Transport in Porous Media and Fractured Rock: From Classical
457 Methods to Modern Approaches (2011), Wiley-VCH Publishers, Weinheim, Germany.

458 [9] D. L. Kuehne, D. I. Ehman, A. S. Emanuel, and C. F. Magnani, J. Petrol. Technol. 42
459 (1990) 504-512.

460 [10] W. R. Rossen, and C. J. van Duijn, J. Petrol. Sci. Eng. 43 (2004) 99-111.

461 [11] M. Sahimi, Rev.Mod. Phys. 65 (1993) 1393–1534.

462 [12] G. M. Homsy, Ann. Rev. Fluid Mech. 19 (1987) 271-311.

463 [13] Y. B. Chang, M. Lim, G. Pope, and K. Sepehrnoori, SPE Reservoir Eng. 9 (1994) 208-
464 216, SPE 22654.

465 [14] A. Andrianov, R. Farajzadeh, M. Mahmoodi Nick, M. Talanana, and P. L. J. Zitha, Ind.
466 Eng. Chem. Res. 51 (2012) 2214-2226.

467 [15] F. Llave, F.H. Chung, R. Louvier, and D. Hudgins, Foams as mobility control agents for
468 oil recovery by gas displacement, SPE/DOE Enhanced Oil Recovery Symposium, (1990),
469 Tulsa, OK, SPE 20245-MS.

470 [16] C.A. Conn, K. Ma, G. J. Hirasaki, and S. L. Biswal , Lab Chip, 14 (2014) 3968-3977.

471 [17] M. Simjoo, Y. Dong, A. Andrianov, M. Talanana, and P.L.J. Zitha, Ind. Eng. Chem.
472 Res. 52 (2013) 6221-6233.

473 [18] T. Blaker, M. G. Aarra, A. Skauge, L. Rasmussen, H. K. Celius, H. A. Martinsen, and F.
474 Vassenden, SPE Reserv. Eval. Eng. (2002), Houston,TX, SPE-56478.

475 [19] E. Mas-Hernandez, P. Grassia, N. Shokri, Colloid Surface A: Physicochem. Eng.
476 Aspects. 473 (2015) 123-132.

477 [20] Q. P. Nguyen, A. V. Alexandrov, P. L. Zitha, and P. K. Currie, SPE International
478 Symposium on Formation Damage Control (2000) Lafayette LA, SPE 58799.

[21] S. H. Talebian, R. Masoudi, I. M. Tan, and P. L. J. Zitha (2014), J. Petrol. Sci. Eng. 120 (2014) 202-215.

[22] F. Friedmann, T. Hughes, M. Smith, G. Hild, A. Wilson, and S. Davies, SPE Annual Technical Conference and Exhibition, (1997) San Antonio, TX. SPE 54429.

[23] P. Grassia, E. Mas-Hernández, N. Shokri, S. J. Cox, G. Mishuris, and W. R. Rossen, J. Fluid Mech. 751 (2014) 346-405.

[24] Bernard, G. G., and L. Holm, Soc. Petrol. Eng. J. 4 (1964) 267-274.

[25] G. Hirasaki, and J. Lawson (1985), Soc. Petrol. Eng. J. 25 (1985) 176-190. SPE 12129.

[26] K. Ma, R. Liontas, C. A. Conn, G. J. Hirasaki, and S. L. Biswal, Soft Matter 8 (2012) 10669-10675.

[27] J. Casteel, and N. Djabbarah, SPE Reservoir Eng. 3 (1988), 1-186. SPE 14392.

[28] H. Bertin, O. Apaydin, L. Castanier, and A. Kovscek, Soc. Petrol. Eng. J. 4 (1999) 75-82. SPE 56009.

[29] A. Falls, J. Musters, and J. Ratulowski, SPE Reservoir Eng, 4 (1989) 155-164, SPE 16048.

[30] S. Marsden, J. Eerligh, R. Albrecht, and A. David, Use of foam in petroleum operations, 7th World Petrol. Congr.(1967) Mexico City, Mexico, WPC 12224.

[31] L. Minssieux, J. Petrol. Technol. 26 (1974) 100-108, SPE 3991.

[32] W. Yan, C. A. Miller, and G. J. Hirasaki, ~~Foam sweep in fractures for enhanced oil recovery~~, Colloid Surfaces A 282 (2006) 348-359.

[33] R. Ettinger, and C. Radke, SPE Reservoir Eng. 7 (1992) 83-90, SPE 19688.

500 [34] S. Vitoonkijvanich, A. M. AlSofi and M. J. Blunt. Int. J. Greenh. Gas Con. 33 (2015)
501 113-121.

502 [35] J. Gauteplass, K. Chaudhary, A. R. Kovscek and M. A. Fernø, Colloid Surfaces A. 468
503 (2015) 184-192.

504 [36] E. Basheva, S., D. Ganchev, N. D. Denkov, K. Kasuga, N. Satoh, and K. Tsujii,
505 Langmuir 16 (1999) 1000-1013.

506 [37] K. Osei-Bonsu, N. Shokri, and P. Grassia (2015), Colloid Surface A: Physicochem. Eng.
507 Aspects 481 (2015) 514–526.

508 [38] W. T. Osterloh and M. Jante, SPE/DOE Enhanced Oil Recovery Symposium (1992)
509 Tulsa, OK. SPE 24179.

510 [39] A. M. Kraynik, Ann. Rev. Fluid Mech. 20 (1988) 325-357.

511 [40] D. Weaire, and S. Hutzler, The Physics of Foam (1999), Oxford University Press.

512 [41] I. Cantat, Phys Fluids. 25 (2013) 031303.

513 [42] I. Cantat, N. Kern, and R. Delannay, EPL. 65 (2004) 726-732.

514 [43] A. H. Falls, G. J. Hirasaki, T. W. Patzek, D. A. Gauglitz, D. D. Miller, and T.
515 Ratulowski, SPE Reservoir Eng. 3 (1988) 884-892, SPE 14961.

516 [44] I. Cantat, and R. Delannay, Phys. Rev. E 67 (2003) 031501.

517 [45] R. Farajzadeh, A. Andrianov, R. Krastev, G. J. Hirasaki, and W. R. Rossen, Adv.
518 Colloid Interface Sci. 183–184 (2012) 1-13.

519 [46] L. L. Schramm, and F. Wassmuth, Foams: Basic Principles, in Foams: Fundamentals
520 and Applications in the Petroleum Industry, ACS (1994) 3-45.

521 [47] B.J. Mitchell, Test data fill theory gap on using foam as a drilling fluid. Oil Gas J. 6
522 (1971) 96-100.

523 [48] Z. Khatib, G. Hirasaki and A. Falls, SPE Reservoir Eng. 3 (1988) 919-926, SPE 15442